ISSN 1674-1056
http://cpb.iphy.ac.cn
http://iopscience.iop.org/cpb
中国物理 B
Chinese Physics
中国物理 Chinese Physics B

Epitaxial fabrication of two-dimensional $TiTe_2$ monolayer on Au(111) substrate with Te as buffer layer

Zhipeng Song(宋志朋), Bao Lei(雷宝), Yun Cao(曹云), Jing Qi(戚竞), Hao Peng(彭浩), Qin Wang(汪琴), Li Huang(黄立), Hongliang Lu(路红亮), Xiao Lin(林晓), Ye-Liang Wang(王业亮), Shixuan Du(杜世萱), Hong-Jun Gao(高鸿钧)

Citation: Chin. Phys. B . 2019, 28(5): 056801. **doi:** 10.1088/1674-1056/28/5/056801
Journal homepage: http://cpb.iphy.ac.cn; http://iopscience.iop.org/cpb

What follows is a list of articles you may be interested in

Controllable fabrication of self-organized nano-multilayers in copper-carbon films

Wei-Qi Wang(王伟奇), Li Ji(吉利), Hong-Xuan Li(李红轩), Xiao-Hong Liu(刘晓红), Hui-Di Zhou(周惠娣), Jian-Min Chen(陈建敏)

Chin. Phys. B . 2019, 28(3): 036802. **doi:** 10.1088/1674-1056/28/3/036802

High quality $PdTe_2$ thin films grown by molecular beam epitaxy

En Li(李恩), Rui-Zi Zhang(张瑞梓), Hang Li(李航), Chen Liu(刘晨), Geng Li(李更), Jia-Ou Wang(王嘉鸥), Tian Qian(钱天), Hong Ding(丁洪), Yu-Yang Zhang(张余洋), Shi-Xuan Du(杜世萱), Xiao Lin(林晓), Hong-Jun Gao(高鸿钧)

Chin. Phys. B . 2018, 27(8): 086804. **doi:** 10.1088/1674-1056/27/8/086804

Effect of hydroxyl on dye-sensitized solar cells assembled with TiO_2 nanorods

Lijian Meng(孟立建), Tao Yang(杨涛), Sining Yun(云斯宁), Can Li(李灿)

Chin. Phys. B . 2018, 27(1): 016802. **doi:** 10.1088/1674-1056/27/1/016802

Image potential states mediated STM imaging of cobalt phthalocyanine on NaCl/Cu(100)

Qinmin Guo(郭秦敏), Zhihui Qin(秦志辉), Min Huang(黄敏), Vladimir N. Mantsevich , Gengyu Cao(曹更玉)

Chin. Phys. B . 2016, 25(3): 036801. **doi:** 10.1088/1674-1056/25/3/036801

Stabilization variation of organic conductor surfaces induced by π–π stacking interactions

Dou Rui-Fen,Lin Feng,Liu Fu-Wei,Sun Yi,Yang Ji-Yong,Lin Bing-Fa,He Lin,Xiong Chang-Min,Nie Jia-Cai

Chin. Phys. B . 2012, 21(5): 056801. **doi:** 10.1088/1674-1056/21/5/056801

RAPID COMMUNICATION

Epitaxial fabrication of two-dimensional $TiTe_2$ monolayer on Au(111) substrate with Te as buffer layer*

Zhipeng Song(宋志朋)[1,†], Bao Lei(雷宝)[1,†], Yun Cao(曹云)[1], Jing Qi(戚竞)[1], Hao Peng(彭浩)[1], Qin Wang(汪琴)[1], Li Huang(黄立)[1], Hongliang Lu(路红亮)[1,‡], Xiao Lin(林晓)[1,3], Ye-Liang Wang(王业亮)[1,2], Shixuan Du(杜世萱)[1,3], and Hong-Jun Gao(高鸿钧)[1,3]

[1] *Institute of Physics and University of Chinese Academy of Sciences, Chinese Academy of Sciences, Beijing* 100190, *China*
[2] *School of Information and Electronics, Beijing Institute of Technology, Beijing* 100081, *China*
[3] *CAS Center for Excellence in Topological Quantum Computation, Beijing* 100049, *China*

(Received 3 February 2019; revised manuscript received 5 March 2019; published online 4 April 2019)

Two-dimensional (2D) materials provide a platform to exploit the novel physical properties of functional nanodevices. Here, we report on the formation of a new 2D layered material, a well-ordered monolayer $TiTe_2$, on a Au(111) surface by molecular beam epitaxy (MBE). Low-energy electron diffraction (LEED) measurements of the samples indicate that the $TiTe_2$ film forms $(\sqrt{3}\times\sqrt{7})$ superlattice with respect to the Au(111) substrate, which has three different orientations. Scanning tunneling microscopy (STM) measurements clearly show three ordered domains consistent with the LEED patterns. Density functional theory (DFT) calculations further confirm the formation of 2H-$TiTe_2$ monolayer on the Au(111) surface with Te as buffer layer. The fabrication of this 2D layered heterostructure expands 2D material database, which may bring new physical properties for future applications.

Keywords: $TiTe_2$, epitaxial fabrication, superlattice, scanning tunneling microscopy (STM), low-energy electron diffraction (LEED)

PACS: 68.37.–d, 68.37.Ef, 81.07.–b, 81.15.Hi **DOI:** 10.1088/1674-1056/28/5/056801

Following the discovery of graphene, tremendous interest in other two-dimensional 2D layered materials has been raised.[1–6] These 2D materials have great potentials in applications of functional devices,[7,8] mainly attributed to their tunable properties with various methods, such as through changing the number of layers, chemical components, or by the formation of heterostructures.[1,9] Among the hundreds of 2D materials, transition metal dichalcogenides (TMDs) have drawn much attention recently due to their novel electronic and optoelectronic properties.[7,10] As one member of TMDs, titanium dichalcogenide compounds have been studied extensively, because they show many amazing physical phenomena like charge-density-wave (CDW) state.[11] For example, a real-space periodic lattice distortion in the CDW state of $TiSe_2$ film with interstitial Ti atoms was observed through the scanning tunneling microscope (STM) measurements.[12] Similar phenomenon and possible formation mechanisms about CDW state in the monolayer $TiTe_2$ are also intriguing.[13] Moreover, the spin–orbit coupling or quantum confinement effects may be observed in these 2D TMDs, these novel phenomena are normally hard to observe in their bulk counterparts.[14–17] Although a large number of TMD materials were fabricated in recent years,[3,18–20] new members of 2D TMD materials family with new structures are still desirable, because it holds new possibilities for novel physics and device applications. 2D $TiTe_2$ with 1T configuration has been fabricated and studied recently,[13,21] but 2D $TiTe_2$ with 2H configuration has not been obtained experimentally so far.

Here, we report the fabrication of 2H-$TiTe_2$ monolayer on a Au(111) substrate. The experiments were carried out in an ultrahigh-vacuum (UHV) molecular beam epitaxy (MBE) system with a base pressure of about 3×10^{-10} mbar. The Au(111) single crystal surface was cleaned by cycles of argon-ion sputtering and annealing to 760 K until it showed clear diffraction spots in the low-energy electron diffraction (LEED) pattern and atomically clean surface in the STM images. The atomic beams of Te and Ti were evaporated to the as-prepared Au(111) substrate from a Knudsen effusion cell and an electron-beam evaporator, respectively. The process for the fabrication of the $TiTe_2$ film was as follows: Te was deposited at first, while the substrate was maintained at 573 K, then Ti was deposited at the same substrate temperature, and finally the substrate was kept at 573 K for 20 min and then slowly cooled down. By these processes, the $TiTe_2$ film formed on the Au(111) surface with Te as the buffer layer. The as-grown samples were characterized *in-situ* by LEED to gain the crys-

*Project supported by the National Key Research & Development Program of China (Grant Nos. 2016YFA0202300 and 2018YFA0305800), the National Natural Science Foundation of China (Grant Nos. 61504149, 61725107, 51572290, and 61622116), the Strategic Priority Research Program of Chinese Academy of Sciences (Grant Nos. XDB30000000 and XDB28000000), the University of Chinese Academy of Sciences, and the CAS Key Laboratory of Vacuum Physics.

†These authors contributed equally to this work.

‡Corresponding author. E-mail: luhl@ucas.ac.cn

© 2019 Chinese Physical Society and IOP Publishing Ltd

tal structure and then transferred to the STM chamber to study the surface morphology and detailed geometric properties.

Density functional theory (DFT) calculations were performed using the Vienna *ab initio* simulation package (VASP). The projector augmented wave (PAW) method was employed and the Perdew–Burke–Ernzernhof (PBE) version of the generalized gradient approximation (GGA) was used. The electronic wave functions were expanded in plane waves with a kinetic energy cutoff of 300 eV. The k-points sampling was $8 \times 3 \times 1$, generated automatically with the origin at the Γ point. The structures were relaxed until the energy and residual force on each atom were smaller than 10^{-5} eV and 0.01 eV/Å, respectively. The STM simulations were performed using the Tersoff–Hamann approach.

Figure 1(a) shows the LEED pattern of the as-prepared sample, and the outer six diffraction spots highlighted by the white circles are originated from the hexagonal lattice of the Au(111) substrate. Apart from these spots, the other diffraction spots can be assigned to the well-ordered film. For more clarity, we sketched a diffraction pattern in reciprocal space as shown in Fig. 1(b), where groups of spots in different sizes and colors are classified in order to describe different structures and domains. Specifically, the diffraction spots are divided to two groups, as shown in Figs. 1(c) and 1(d). Each group of spots is generated by three domains as represented in different colors.

Figures 1(e) and 1(f) show the lattice structures in real space, corresponding to the diffraction spots indicated by the arrows in Figs. 1(c) and 1(d), respectively. The crystalline matrix of the superstructure in Fig. 1(e) is $(1, -1 \mid 2, 3)$. This sketch distinctly shows a commensurate relation between the film and the substrate lattice, which has a superstructure of $(\sqrt{3} \times \sqrt{7})$. As discussed in the following, this structure can be attributed to $TiTe_2$ layer on Au(111) substrate with Te as the buffer layer.

The diffraction spots shown in Fig. 1(d) are generated by a high-order commensurate structure of $(7/4, 1 \mid -3/4, 1)$, as shown in Fig. 1(f). They are probably originated from the Te thin film, because excess Te was deposited in the growth process. The lattice period of this structure in real space is ~ 0.44 nm, which is consistent with the lattice constant of bulk Te. The crystal unit cell has a little distortion to be commensurate with the substrate lattice.

To further investigate the surface structure of the sample, STM was used to characterize the surface morphology in real space. Figure 2(a) shows an STM image of the sample surface, in which three domains can be clearly distinguished, as labeled by α, β, and γ. We can also see that the crystal directions are $30°$, $-30°$, and $90°$. To characterize the surface structure more clearly, we mapped these three domains separately in detail, as demonstrated in Figs. 2(b)–2(d). It is clear that the superstructure is an oblique structure. The unit cell of the superstructure is marked by a black parallelogram, corresponding to $(\sqrt{3} \times \sqrt{7})$ superlattice with respect to the Au(111) substrate, consistent with the LEED patterns.

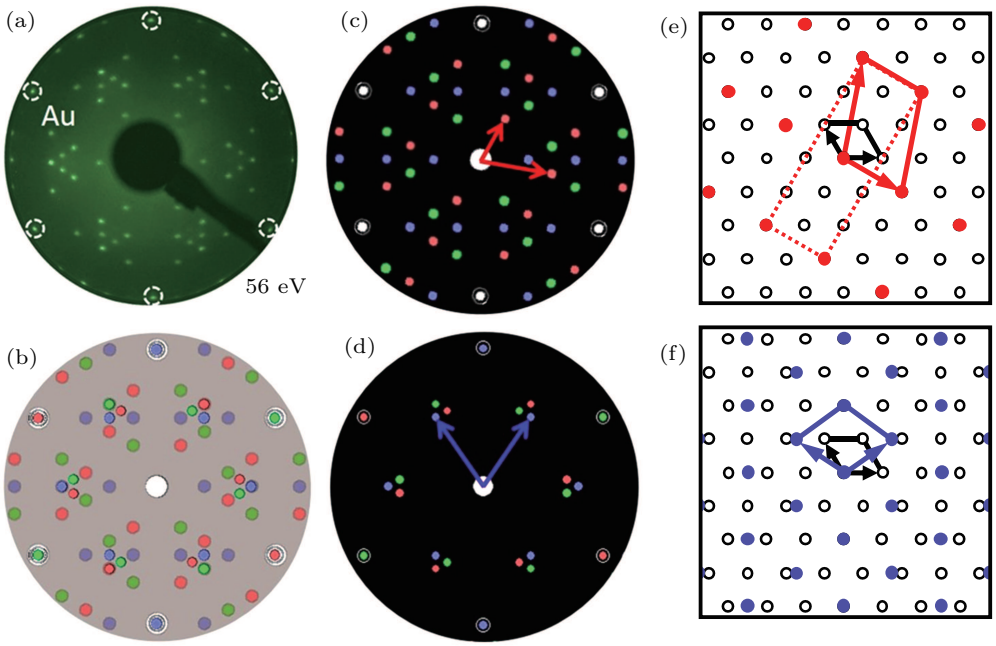


Fig. 1. (a) LEED pattern of $TiTe_2$ superstructure formed on Au(111) surface. The white circles indicate the diffraction spots originated from the Au(111) substrate. The additional diffraction spots are ascribed to the $TiTe_2$ and Te films. (b) Sketch of the diffraction spots shown in (a), which includes two groups of spots as shown in (c) and (d). Each group of spots is generated by three domains as represented in different colors. (e) and (f) Lattice structures in real space, corresponding to the diffraction spots indicated by the arrows in (c) and (d), respectively. These data reveal a superstructure of $(\sqrt{3} \times \sqrt{7})$ as shown in (e) and a high order commensurate structure of $(7/4, 1 \mid -3/4, 1)$ as shown in (f). Black circles in (e) and (f) indicate the lattices of the Au(111) substrate.

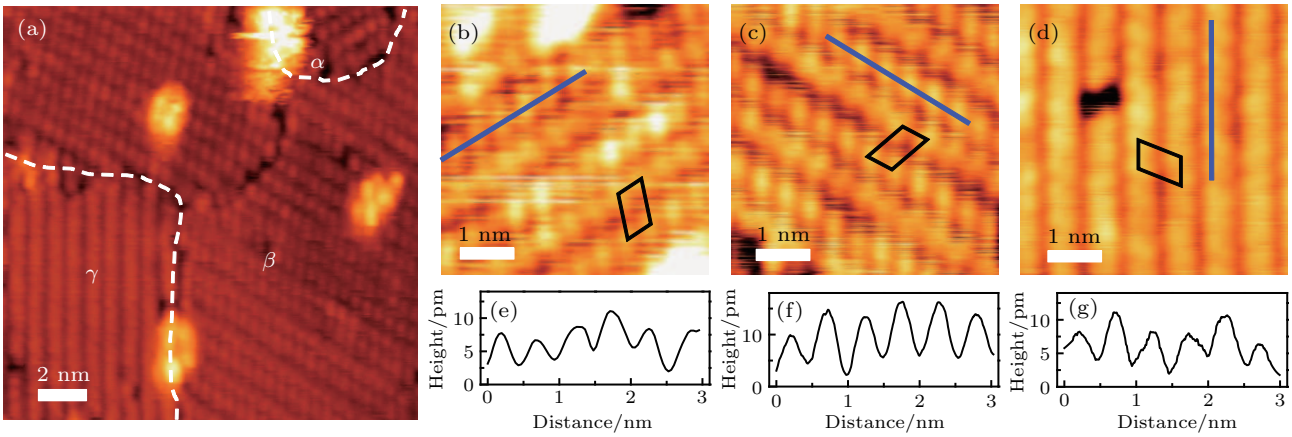


Fig. 2. STM images of the 2D $TiTe_2$ layer formed on the Au(111) surface. (a) STM image showing the three domains, marked as α, β, and γ. (b)–(d) Zoom-in STM images of the α, β, and γ domains in (a). (e)–(g) Line profiles of the purple lines in (b)–(d), respectively, which show periods of 5.0 Å, in agreement with $\sqrt{3}$ times of the Au substrate lattice constant. The sample bias and tunneling current: −10 mV, 40 pA in (a), −0.5 V, 50 pA in (b), −50 mV, 40 pA in (c) and (d).

Figures 2(e)–2(g) are the line profiles along the purple lines in Figs. 2(b)–2(d), in which the period of the superstructure is about 5.0 Å, in agreement with $\sqrt{3}$ times of the Au substrate lattice constant ($\sqrt{3} \times 2.89$ Å = 5.0 Å). These STM images match with the diffraction spots in the LEED pattern with the $(\sqrt{3} \times \sqrt{7})$ structure. The superstructure in Fig. 1(f) deduced from the complicated LEED pattern was not observed in the STM experiments, possibly because STM is a surface-sensitive technique, hard to detect the superstructure underneath the surface layer.

To understand the STM images, we performed DFT-based calculations and simulations. Figure 3(a) shows a stable structure obtained by the calculations. This is a 2H-$TiTe_2$ monolayer on the Au(111) surface with a buffer Te layer between the $TiTe_2$ film and the substrate, which shows a $(\sqrt{3} \times 5)$ superstructure (red rectangle). The lattice constants of this 2H-$TiTe_2$ are about $a = 3.69$ Å and $b = 3.28$ Å, a little smaller than that of freestanding 1T-$TiTe_2$ of 3.76 Å,[22] which may be induced by the substrate. In order to accommodate the in-plane compression of the lattice constants, the distance between Te atomic layers in the $TiTe_2$ sandwich structure is elongated in the z direction to be 4.13 Å, while this distance in freestanding 1T-$TiTe_2$ is only 3.47 Å.[22] Figure 3(b) is the simulated STM image of this relaxed structure. Besides $(\sqrt{3} \times 5)$ superstructure (red rectangle), $(\sqrt{3} \times \sqrt{7})$ structure (black parallelogram) is also displayed, because the electronic states of the top Te atoms merge. Figure 3(c) is an experimentally obtained high resolution STM image, which shows a good agreement with the simulated result in Fig. 3(b), indicating the validity of the structural model with 2H-$TiTe_2$ monolayer on Au(111) and Te as buffer layer. We also calculated the structure with 1T-$TiTe_2$ as the top layer and simulated the STM image. However, the results are inconsistent with the $(\sqrt{3} \times \sqrt{7})$ superstructure observed in the LEED and STM experiments.

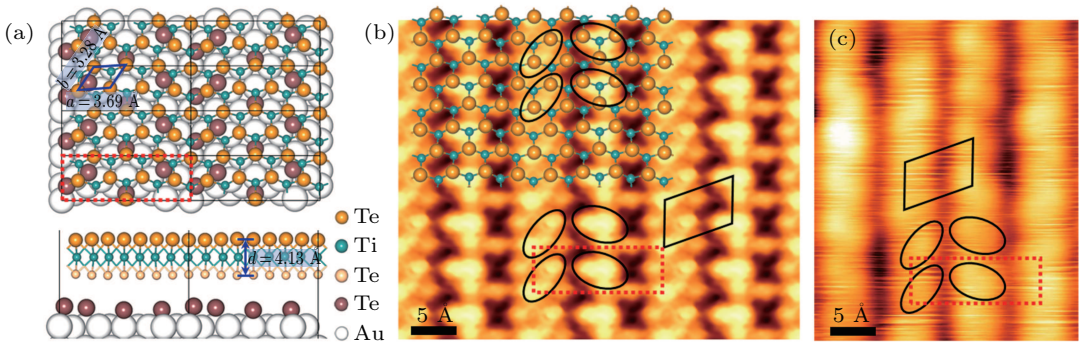


Fig. 3. (a) Top and side views of the relaxed atomic model of the $TiTe_2$/Te/Au(111) structure showing a $(\sqrt{3} \times 5)$ superstructure (red rectangle). (b) Simulated STM image of the configuration in (a), showing both $(\sqrt{3} \times 5)$ (red rectangle) and $(\sqrt{3} \times \sqrt{7})$ (black parallelogram) superstructures. The atomic model is overlapped on the top for comparison. (c) High resolution STM image (−50 mV, 40 pA) showing two superstructures.

In summary, we have successfully synthesized 2D $TiTe_2$ layer with 2H configuration, which is a new member of the TMDs family, on a Au(111) surface by MBE method. STM and LEED characterizations combined with DFT calculations demonstrate the formation of $(\sqrt{3} \times \sqrt{7})$ superlattice of the $TiTe_2$ monolayer with Te as buffer layer on the Au(111) substrate. This work may help to enrich the understanding of the superstructures of 2D layered materials and provides a new

candidate in 2D materials family to explore novel physical properties and related applications.

References

[1] Novoselov K S, Mishchenko A, Carvalho A and Castro Neto A H 2016 *Science* **353** aac9439

[2] Pan Y, Zhang L Z, Huang L, Li L F, Meng L, Gao M, Huan Q, Lin X, Wang Y L, Du S X, Freund H J and Gao H J 2014 *Small* **10** 2215

[3] Lin X, Lu J C, Shao Y, Zhang Y Y, Wu X, Pan J B, Gao L, Zhu S Y, Qian K, Zhang Y F, Bao D L, Li L F, Wang Y Q, Liu Z L, Sun J T, Lei T, Liu C, Wang J O, Ibrahim K, Leonard D N, Zhou W, Guo H M, Wang Y L, Du S X, Pantelides S T and Gao H J 2017 *Nat. Mater.* **16** 717

[4] Dong L, Wang A, Li E, Wang Q, Li G, Huan Q and Gao H J 2019 *Chin. Phys. Lett.* **36** 028102

[5] Meng L, Wang Y L, Zhang L Z, Du S X and Gao H J 2015 *Chin. Phys. B* **24** 086803

[6] Huang L, Li G, Zhang Y Y, Bao L H, Huan Q, Lin X, Wang Y L, Guo H M, Shen C M, Du S X and Gao H J 2018 *Acta Phys. Sin.* **67** 126801 (in Chinese)

[7] Wang Q H, Kalantar-Zadeh K, Kis A, Coleman J N and Strano M S 2012 *Nat. Nanotechnol.* **7** 699

[8] Lu J, Bao D L, Qian K, Zhang S, Chen H, Lin X, Du S X and Gao H J 2017 *ACS Nano* **11** 1689

[9] Terrones H, Lopez-Urias F and Terrones M 2013 *Sci. Rep.* **3** 1549

[10] Chhowalla M, Shin H S, Eda G, Li L J, Loh K P and Zhang H 2013 *Nat. Chem.* **5** 263

[11] Reshak A H and Auluck S 2003 *Phys. Rev. B* **68** 245113

[12] Hildebr, B, Jaouen T, Mottas M L, Monney G, Barreteau C, Giannini E, Bowler D R and Aebi P 2018 *Phys. Rev. Lett.* **120** 136404

[13] Chen P, Pai W W, Chan Y H, Takayama A, Xu C Z, Karn A, Hasegawa S, Chou M Y, Mo S K, Fedorov A V and Chiang T C 2017 *Nat. Commun.* **8** 516

[14] Mak K F, He K, Shan J and Heinz T F 2012 *Nat. Nanotechnol.* **7** 494

[15] Mak K F, Lee C, Hone J, Shan J and Heinz T F 2010 *Phys. Rev. Lett.* **105** 136805

[16] Splendiani A, Sun L, Zhang Y, Li T, Kim J, Chim C Y, Galli G and Wang F 2010 *Nano Lett.* **10** 1271

[17] Zhang Y, Chang T R, Zhou B, Cui Y T, Yan H, Liu Z, Schmitt F, Lee J, Moore R, Chen Y, Lin H, Jeng H T, Mo S K, Hussain Z, Bansil A and Shen Z X 2013 *Nat. Nanotechnol.* **9** 111

[18] Bonilla M, Kolekar S, Ma Y, Diaz H C, Kalappattil V, Das R, Eggers T, Gutierrez H R, Manh-Huong P and Batzill M 2018 *Nat. Nanotechnol.* **13** 289

[19] Shao Y, Song S, Wu X, Qi J, Lu H, Liu C, Zhu S, Liu Z, Wang J, Shi D, Du S, Wang Y and Gao H J 2017 *Appl. Phys. Lett.* **111** 113107

[20] Xi X, Zhao L, Wang Z, Berger H, Forro L, Shan J and Mak K F 2015 *Nat. Nanotechnol.* **10** 765

[21] Guster B, Robles R, Pruneda M, Canadell E and Ordejon P 2019 *2d Materials* **6** 015027

[22] Mounet N, Gibertini M, Schwaller P, Campi D, Merkys A, Marrazzo A, Sohier T, Castelli I E, Cepellotti A, Pizzi G and Marzari N 2018 *Nat. Nanotechnol.* **13** 246